

Anisotropic Durgapal-Fuloria Neutron Stars in $f(\mathcal{R}, T^2)$ Gravity

Tayyab Naseer ^{*}, M. Sharif [†], Sana Manzoor [‡] and Arooj Fatima [§]
Department of Mathematics and Statistics, The University of Lahore,
1-KM Defence Road Lahore-54000, Pakistan.

Abstract

The main purpose of this paper is to obtain physically stable stellar models coupled with anisotropic matter distribution in the context of $f(\mathcal{R}, T^2)$ theory. For this, we consider a static spherical geometry and formulate modified field equations containing various unknowns such as matter determinants and metric potentials. We then obtain a unique solution to these equations by employing Durgapal-Fuloria ansatz possessing a constant doublet. We also use matching criteria to calculate the values of these constants by considering the Schwarzschild exterior spacetime. Two different viable models of this modified theory are adopted to analyze the behavior of effective matter variables, anisotropy, energy conditions, compactness and redshift in the interiors of Her X-1, PSR J0348-0432, LMC X-4, SMC X-1, Cen X-3, and SAX J 1808.4-3658 star candidates. We also check the stability of these models by using three different physical tests. It is concluded that our considered stars satisfy all the physical requirements and are stable in this modified gravity for the considered parametric values.

Keywords: Modified theory; Stellar objects; Anisotropy.

PACS: 04.50.Kd; 97.60.Jd; 97.10.-q; 98.35.Ac.

^{*}tayyabnaseer48@yahoo.com; tayyab.naseer@math.uol.edu.pk

[†]msharif.math@pu.edu.pk

[‡]sanamanzoormath@gmail.com

[§]arooj3740@gmail.com

1 Introduction

General Relativity (GR) describes the fundamental forces that govern the motion of objects in the universe, particularly, in the presence of massive structures like stars and planets. This is an essential part of the foundation of modern cosmology and our understanding of cosmic structure as well as evolution. Singularities are the key issues in GR because they represent points in spacetime where the curvature becomes infinite and the laws of physics break down. In specific scenarios, singularities are predicted to appear such as at the core of a black hole or during the initial moments of the big bang when energy densities and curvatures reach exceedingly high levels. Consequently, the predictions made by GR regarding extreme energy levels, particularly, the singularity linked to the origin of the universe (the big bang) lose their validity. A reliable explanation of these unusual instances has been provided by modified theories of GR. Different approaches, i.e., higher-dimensional gravity [1], $f(\mathcal{R})$ [2, 3], $f(\mathcal{R}, T)$ [4]-[6] and scalar-tensor theories [7] have been proposed and examined as a result of this pursuit. These alternative theories enhance our understanding of how gravity operates in scenarios where classical GR proves insufficient.

In 2014, Katirci and Kavuk [8] presented a significant modification to GR by including self-contraction of the energy-momentum tensor, i.e., $(T_{\xi\psi}T^{\xi\psi} = T^2)$ into the action. They named this modified theory as “energy-momentum squared gravity” (EMSG) or $f(\mathcal{R}, T^2)$ theory. This theory potentially resolved significant cosmological puzzles as it has been suggested as a candidate for explaining the observed accelerated expansion of the universe. It also offers a promising approach to understand the early-time universe in a more comprehensive manner. An important feature of this theory is its ability to calculate the additional acceleration that affects the perihelion of Mercury. This is accomplished by determining the Newtonian limit of the model. The field equations of this theory involve squared and product terms of the matter variables, helping in studying diverse cosmological scenarios. Another noteworthy feature of this theory is that the traditional conservation of energy and momentum may not hold due to the interaction between matter and curvature that introduces an additional force. As a result, the trajectory of a test particle differs from the standard geodesic path predicted by GR.

This modified theory has sparked significant interest in the fields of astrophysics and cosmology. Researchers have explored its implications for various

astronomical structures, seeking to understand how this novel framework alters our understanding of the universe evolution and behavior, particularly, in extreme conditions where classical physics breaks down. The homogeneous and isotropic spacetime has been studied in the modified $f(\mathcal{R}, T^2)$ theory and observed that there was a possibility of bounce at early-times instead of the big bang singularity. Board and Barrow [9] found an exact solution for isotropic universe and discussed their behavior with respect to the early and late-time cosmic evolution in this theory. Moraes and Sahoo [10] proposed the existence of non-exotic matter wormholes in this framework. The effect of this modified theory of gravity on neutron stars and nuclear properties of the matter distribution has been extensively discussed [11].

Celestial objects, particularly, stars are assumed as a fundamental element in shaping the composition of galaxies within our universe. The intricate structure of these celestial bodies has captivated the attention of numerous astrophysicists, who have dedicated their efforts to analyze the various stages of their evolution. The gravitational collapse marks the end of a star, resulting in new astrophysical structures such as black holes, neutron stars and white dwarfs depending on the mass of the dying star. Neutron stars, in particular, have garnered significant attention due to their fascinating structural characteristics and evolutionary stages. Numerous researchers have explored these structures and their formation. Dev and Gleiser [12] analyzed the surface redshift and stability of self-gravitating stars. Mak and Harko [13] obtained a class of exact solutions, describing static spherically symmetric stellar configuration. Kalam et al. [14] used the Krori-Barua metric to study the physical characteristics of strange stars. A large body of literature exists on the discussion of different properties of neutron stars [15, 16]. Singh and Pant [17] found a class of exact solutions for anisotropic stars and examined that all the energy conditions are satisfied for these solutions. Maurya and Tello-Ortiz [18] examined the anisotropy and surface redshift of celestial bodies in the modified $f(\mathcal{R})$ theory. Sharif and Naseer [19]-[21] employed a particular EoS to examine the stability of various neutron star candidates in a non-minimal gravity. Some other approaches have also been used in the literature to discuss the neutron star models [22]-[29].

A family of isotropic solutions, whether exact or approximate, does not have physical relevance and is not aligned with what we observe in astrophysical phenomena [30]-[32]. Researchers have found compelling evidences that various intriguing physical phenomena can lead to local deviations from uniformity and isotropy. These deviations can occur within both low and

high density regimes. For example, in the later scenario, such as the cores of extremely compact astrophysical objects where matter is packed incredibly dense (densities even higher than that of the nuclear density $3 \times 10^{17} \text{ kg/m}^3$), exhibits anisotropic behavior [33]. Anisotropic behavior in these high-density objects occurs because the pressure inside them does not act uniformly in all directions. Instead, it can be divided into two distinct components, i.e., radial and transverse. Anisotropy in fluid pressure often emerges from various factors and physical conditions within a system such as the mixture of fluids of different types, rotation, viscosity, the existence of a solid core, the presence of a superfluid or a magnetic field [13]. Researchers have extensively explored these sources of anisotropy in higher dimensions [34]-[38]. A body of literature is present that discusses anisotropic neutron stars using different approaches [39, 40] as well as attempts to understand the anisotropic pressure in such stellar objects from matter/geometric aspects [41]-[44]. Some other recent neutron stars observation reports from different collaborators can be seen in [45]-[48]. Hence, it becomes appealing to apply relativistic principles to understand how the fundamental forces and particles interact, and affect the behavior of astrophysical objects, contributing to broader our understanding of the cosmos.

Durgapal and Fuloria [49] presented a viable perfect fluid solution to characterize the incredibly dense configurations of stellar objects like neutron stars. Their work provided a theoretical framework that not only accurately represents the extreme conditions within neutron stars but also ensures the stability of this solution against radial perturbations. Later, this solution was extended for anisotropic as well as charged stellar configurations. Maurya et al. [50] used this ansatz to obtain viable star models coupled with the anisotropic matter distribution. Komathiraj et al. [51] generalized the isotropic Durgapal-Fuloria solution for anisotropic charged stellar objects and analyzed their physical properties. Maurya et al. [52] formulated the complexity-free anisotropic generalization of such an isotropic model through the extended geometric deformations.

In this paper, we analyze anisotropic neutron stars with static spherically symmetric interior in $f(\mathcal{R}, T^2)$ theory. In section **2**, we take Durgapal-Fuloria ansatz and construct the corresponding field equations. In order to calculate the values of unknown constants, we use matching conditions between the interior and the Schwarzschild exterior geometries. In sections **3** and **4**, we choose different viable models of this modified theory and explore physical properties of the considered stars. We examine the effective matter variables,

energy bounds, EoS parameters corresponding to the resulting solutions. We also check stability through the sound speed as well as the cracking approach in section 5. Section 6 summarizes our obtained results.

2 $f(\mathcal{R}, \mathbb{T}^2)$ Theory

The Einstein-Hilbert action takes the form in EMSG scenario (for $\kappa = 1$) as [11]

$$I = \int \sqrt{-g} \left\{ \frac{f(\mathcal{R}, \mathbb{T}^2)}{2} + L_m \right\} d^4x, \quad (1)$$

where L_m defines the matter Lagrangian density of the fluid configuration and $g = |g_{\xi\psi}|$ with $g_{\xi\psi}$ being the metric tensor. The field equations corresponding to the above modified action are formulated as

$$\mathcal{R}_{\xi\psi} f_{\mathcal{R}} + g_{\xi\psi} \nabla_{\xi} \nabla^{\xi} f_{\mathcal{R}} - \nabla_{\xi} \nabla_{\psi} f_{\mathcal{R}} - \frac{1}{2} g_{\xi\psi} f = \mathbb{T}_{\xi\psi} - \Theta_{\xi\psi} f_{\mathbb{T}^2}, \quad (2)$$

where $f_{\mathbb{T}^2} = \frac{\partial f(\mathcal{R}, \mathbb{T}^2)}{\partial \mathbb{T}^2}$ and $f_{\mathcal{R}} = \frac{\partial f(\mathcal{R}, \mathbb{T}^2)}{\partial \mathcal{R}}$. Also, $\mathbb{T}_{\xi\psi}$ is the usual energy-momentum tensor and

$$\Theta_{\xi\psi} = 2\mathbb{T}_{\xi}^{\zeta} \mathbb{T}_{\psi\zeta} - 2L_m \left(\mathbb{T}_{\xi\psi} - \frac{1}{2} g_{\xi\psi} \mathbb{T} \right) - \frac{4\partial^2 L_m}{\partial g^{\xi\psi} \partial g^{\zeta\eta}} \mathbb{T}^{\zeta\eta} - \mathbb{T} \mathbb{T}_{\xi\psi}. \quad (3)$$

Rearranging Eq.(2), we obtain

$$G_{\xi\psi} = \mathcal{R}_{\xi\psi} - \frac{1}{2} \mathcal{R} g_{\xi\psi} = \mathbb{T}_{\xi\psi}^{eff}, \quad (4)$$

where the EMSG corrections are given by

$$\mathbb{T}_{\xi\psi}^{eff} = \frac{1}{f_{\mathcal{R}}} \left[\mathbb{T}_{\xi\psi} + \nabla_{\xi} \nabla_{\psi} f_{\mathcal{R}} - g_{\xi\psi} \nabla_{\xi} \nabla^{\xi} f_{\mathcal{R}} + \frac{1}{2} g_{\xi\psi} (f - \mathcal{R} f_{\mathcal{R}}) - \Theta_{\xi\psi} f_{\mathbb{T}^2} \right]. \quad (5)$$

We consider that the hypersurface distinguishes the interior and exterior region of a self-gravitating geometry. In order to study the physical properties of stellar structures, we assume a static sphere as the interior metric

$$ds_-^2 = -e^{\tau} dt^2 + e^{\nu} dr^2 + r^2 (d\theta^2 + \sin^2 \theta d\phi^2), \quad (6)$$

where $\tau = \tau(r)$ and $\nu = \nu(r)$. The energy-momentum tensor plays a crucial role in the modeling of celestial objects because it specifies the interior matter

distribution. In the realm of astrophysics, the study of compact neutron-like stars has been a fascinating area of exploration, providing valuable insights into the fundamental nature of matter under extreme conditions. Traditional approaches have predominantly focused on isotropic models to understand these dense celestial objects. However, the limitations of isotropic models become evident when faced with the intricacies of celestial systems. This motivation seeks to highlight the imperative shift towards investigating anisotropic stars within the framework of modified theories, presenting a unique and promising avenue for advancing our understanding of the cosmos. Since we aim to model anisotropic star candidates, the corresponding energy-momentum tensor has the form

$$T_{\xi\psi} = \rho U_{\xi} U_{\psi} + P_r V_{\xi} V_{\psi} + P_t (U_{\xi} U_{\psi} - V_{\xi} V_{\psi} + g_{\xi\psi}), \quad (7)$$

where the triplet (P_t, P_r, ρ) symbolizes the tangential/radial pressures and the energy density, respectively. Also, U_{ξ} is the four-velocity and V_{ξ} indicates the four-vector. It is mentioned here that a large body of literature formulates physically relevant models for the Lagrangian $L_m = \frac{P_r + 2P_t}{3}$, thus we consider it in this case. Joining this with the field equations (4), we get

$$\begin{aligned} \rho^{eff} &= \frac{1}{f_{\mathcal{R}}} \left[\rho + \frac{\mathcal{R}f_{\mathcal{R}} - f}{2} + f_{T^2} \left\{ \left(\frac{P_r + 2P_t}{3} \right) (\rho + 2P_t + P_r) \right. \right. \\ &\quad \left. \left. + \rho^2 + 2\rho P_t + \rho P_r \right\} + \frac{1}{e^{\nu}} \left\{ f''_{\mathcal{R}} - \left(\frac{\nu'}{2} - \frac{2}{r} \right) f'_{\mathcal{R}} \right\} \right], \end{aligned} \quad (8)$$

$$\begin{aligned} P_r^{eff} &= \frac{1}{f_{\mathcal{R}}} \left[P_r - \frac{\mathcal{R}f_{\mathcal{R}} - f}{2} + \left\{ \left(\frac{P_r + 2P_t}{3} \right) (P_r - 2P_t + \rho) \right. \right. \\ &\quad \left. \left. - (P_r^2 - 2P_r P_t + \rho P_r) \right\} f_{T^2} - \frac{1}{e^{\nu}} \left(\frac{2}{r} + \frac{\tau'}{2} \right) f'_{\mathcal{R}} \right], \end{aligned} \quad (9)$$

$$\begin{aligned} P_t^{eff} &= \frac{1}{f_{\mathcal{R}}} \left[P_t - \frac{\mathcal{R}f_{\mathcal{R}} - f}{2} - \frac{1}{e^{\nu}} \left\{ f'_{\mathcal{R}} \left(\frac{\tau'}{2} + \frac{1}{r} - \frac{\nu'}{2} \right) + f''_{\mathcal{R}} \right\} \right. \\ &\quad \left. + \left\{ \left(\frac{P_r + 2P_t}{3} \right) (\rho - P_r) + P_r P_t - \rho P_t \right\} f_{T^2} \right]. \end{aligned} \quad (10)$$

We observe that there are five unknowns $(\nu, \tau, \rho, P_r, P_t)$ in the above three equations, making them difficult to solve. In order to find a unique solution to these equations, we adopt a particular form of the metric components in the following. The singularity-free Durgapal-Fuloria ansatz is given by [49]

Table 1: Estimated data of various stellar objects and their corresponding calculated values of constants.

Star models	$M(M_{\odot})$	R	M/R	A	B
Her X-1 [53]	0.85	8.1	0.1049	0.606611	0.00104111
PSR J0348-0432 [53]	2.1	10.06	0.20874	0.3281	0.00152477
LMC X-4 [54]	1.29	8.831	0.14607	0.483925	0.00127895
SMC X-1 [54]	1.04	9.34	0.1113	0.58638	0.000836898
Cen X-3 [54]	1.49	10.8	0.1380	0.506798	0.000799845
SAX J 1808.4-3658 [55]	1.44	7.07	0.2036	0.339377	0.00299192

$$e^{\tau(r)} = A(1 + Br^2)^4, \quad (11)$$

$$e^{\nu(r)} = \frac{7(1 + Br^2)^2}{7 - B^2r^4 - 10Br^2}, \quad (12)$$

where A and B are constants. We find their values by matching the interior spacetime with the exterior geometry at the spherical junction. Thus, we choose the Schwarzschild spacetime representing solution to the field equations in vacuum as

$$ds_+^2 = -jdt^2 + \frac{1}{j}dr^2 + r^2(d\theta^2 + \sin^2\theta d\phi^2), \quad (13)$$

where $j = 1 - \frac{2M}{r}$ and M being the total exterior mass. In traditional GR, the exterior solution indeed simplifies to the Schwarzschild metric when the source terms vanish. However, in modified gravity theories, especially those incorporating additional curvature and energy-momentum tensor terms, the correspondence to the Schwarzschild solution might not be as straightforward, and additional geometric terms may persist. Several researchers discussed that even when matter and pressure tend towards zero, certain geometrical terms may persist due to the intricate coupling introduced by the modified gravity frameworks [56, 57]. Some different but interesting works are [58]-[61]. The smooth matching at the surface boundary ($\Sigma : r = R$) yields

$$A = \frac{R - 2M}{R(1 + BR^2)^4}, \quad (14)$$

$$B = \frac{6R^3 - 7MR^2 - 2\sqrt{9R^6 - 14MR^5}}{7MR^4 - 4R^5}. \quad (15)$$

We consider estimated masses and radii of six different star candidates in Table 1 that would be helpful to calculate the above two constants and thus

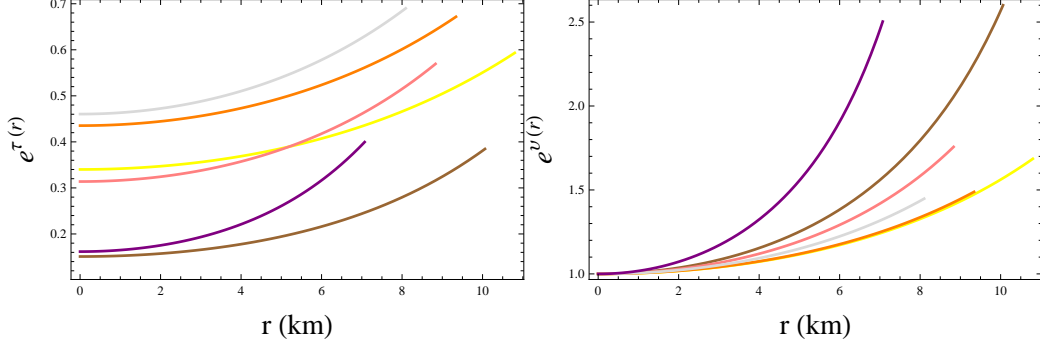


Figure 1: Metric potentials versus r corresponding to SMC X-1 (orange), PSR J0348-0432 (brown), Her X-1 (gray), LMC X-4 (cyan), Cen X-3 (yellow) and SAX J 1808.4-3658 (purple).

to plot the physical characteristics of the resulting solution. We also provide a constant doublet (A, B) corresponding to each candidate in Table 1. The components (11) and (12) are plotted in Figure 1, showing non-singular and increasing profile everywhere in the considered range of celestial objects. Since the matter variables are appeared up to quadratic order in the field equations, their explicit expressions cannot be obtained. Therefore, we consider $\rho = \frac{3m}{4\pi r^3}$, $P_r = \frac{\rho}{3}$ and $P_t = (\zeta + 1)P_r$ with $m = m(r)$ being the interior mass and $\zeta > 0$. It must be mentioned here that the pressure anisotropy in the interior of a self-gravitating model must be positive in order to produce enough outward pressure to counterbalance the inward gravitational force. We observe that the above considered form of the anisotropic function is aligned with such scenarios. Inserting these assumptions in the field equations, they become

$$\begin{aligned} \rho^{eff} &= \frac{1}{f_{\mathcal{R}}} \left[\frac{3m}{4\pi r^3} + \frac{m^2}{12\pi^2 r^6} (\zeta^2 + 9\zeta + 18) f_{\mathbb{T}^2} + \frac{7 - B^2 r^4 - 10Br^2}{7(1 + Br^2)^2} \right. \\ &\quad \times \left. \left\{ f_{\mathcal{R}}'' - \left(\frac{8Br(-3 + Br^2)}{(1 + Br)(-7 + 10Br^2 + B^2 r^4)} - \frac{2}{r} \right) f_{\mathcal{R}}' \right\} - \frac{f - \mathcal{R}f_{\mathcal{R}}}{2} \right], \end{aligned} \quad (16)$$

$$\begin{aligned} P_r^{eff} &= \frac{1}{f_{\mathcal{R}}} \left[\frac{m}{4\pi r^3} + \frac{m^2}{12\pi^2 r^6} (\zeta - \zeta^2) f_{\mathbb{T}^2} - \frac{7 - B^2 r^4 - 10Br^2}{7(1 + Br^2)^2} \right. \\ &\quad \times \left. \left(\frac{2}{r} + \frac{4Br}{1 + Br^2} \right) f_{\mathcal{R}}' + \frac{1}{2} (f - \mathcal{R}f_{\mathcal{R}}) \right], \end{aligned} \quad (17)$$

$$\begin{aligned}
P_t^{eff} &= \frac{1}{f_{\mathcal{R}}} \left[(1 + \varsigma) \frac{m}{4\pi r^3} - \frac{m^2 \varsigma}{24\pi^2 r^6} f_{T^2} + \frac{1}{2} (f - \mathcal{R} f_{\mathcal{R}}) - \frac{7 - B^2 r^4 - 10Br^2}{7(1 + Br^2)^2} \right. \\
&\quad \left. \times \left\{ f_{\mathcal{R}}'' + \left(\frac{4Br}{1 + Br^2} - \frac{8Br(-3 + Br^2)}{(1 + Br)(-7 + 10Br^2 + B^2 r^4)} + \frac{1}{r} \right) f_{\mathcal{R}}' \right\} \right].
\end{aligned} \tag{18}$$

3 Different Models of Modified Gravity

The inclusion of multivariate functions in the field equations (16)-(18) makes this theory different from others, and thus these equations are much complicated to be solved. In order to tackle this situation, we focus on two particular models within the framework of EMSG theory. Since such kind of matter-geometry coupled theories can be discussed by taking either minimal or non-minimal models, we specifically assume the former model in which geometry and matter distribution are independent of each other. Such models in this theory can be provided by

$$f(\mathcal{R}, T^2) = f_1(\mathcal{R}) + f_2(T^2). \tag{19}$$

Several EMSG models have been discussed in the literature by taking different forms of $f_1(\mathcal{R})$ and $f_2(T^2)$. In the following, we shall discuss two different forms of $f_1(\mathcal{R})$ while fixing $f_2(T^2) = \beta T^2$ with β being an arbitrary constant.

Model I

Here, we adopt a particular form of $f_1(\mathcal{R})$ proposed by Starobinsky [62]. Thus, the model (19) takes the form

$$f(\mathcal{R}, T^2) = \mathcal{R} + \alpha \mathcal{R}^2 + \beta T^2, \tag{20}$$

where α is a non-negative model parameter. Notice that $\beta = 0$ reduces the results of this theory to those in $f(\mathcal{R})$ framework. Moreover, $\alpha = 0 = \beta$ leads them to GR. Equations (16)-(18) become under this model as

$$\begin{aligned}
\rho^{eff} &= \frac{1}{1 + 2\alpha \mathcal{R}} \left[\frac{3m}{4\pi r^3} + \frac{\beta m^2}{48\pi^2 r^6} (54 + 33\varsigma + 4\varsigma^2) + \frac{7 - B^2 r^4 - 10Br^2}{7(1 + Br^2)^2} \right. \\
&\quad \left. \times \left\{ 2\alpha \mathcal{R}'' - 2\alpha \mathcal{R}' \left(\frac{8Br(-3 + Br^2)}{(1 + Br)(-7 + 10Br^2 + B^2 r^4)} - \frac{2}{r} \right) \right\} + \frac{1}{2} \alpha \mathcal{R}^2 \right],
\end{aligned} \tag{21}$$

$$P_r^{eff} = \frac{1}{1+2\alpha\mathcal{R}} \left[\frac{m}{4\pi r^3} + \frac{\beta m^2}{48\pi^2 r^6} (18 + 7\varsigma - 4\varsigma^2) - \frac{7 - B^2 r^4 - 10Br^2}{7(1+Br^2)^2} \right. \\ \left. \times \left(\frac{4Br}{1+Br^2} + \frac{2}{r} \right) 2\alpha\mathcal{R}' - \frac{1}{2}\alpha\mathcal{R}^2 \right], \quad (22)$$

$$P_t^{eff} = \frac{1}{1+2\alpha\mathcal{R}} \left[(1+\varsigma) \frac{m}{4\pi r^3} + \frac{\beta m^2}{16\pi^2 r^6} \left(6 + \frac{1}{3}\varsigma \right) - \frac{7 - B^2 r^4 - 10Br^2}{7(1+Br^2)^2} \right. \\ \left. \times \left\{ 2\alpha\mathcal{R}'' + 2\alpha\mathcal{R}' \left(\frac{4Br}{1+Br^2} - \frac{8Br(-3+Br^2)}{(1+Br)(-7+10Br^2+B^2r^4)} + \frac{1}{r} \right) \right\} \right. \\ \left. - \frac{1}{2}\alpha\mathcal{R}^2 \right]. \quad (23)$$

Model II

In this subsection, we choose another form of $f_1(\mathcal{R})$ as $\mathcal{R} - \omega v \tanh\left(\frac{\mathcal{R}}{\omega}\right)$ with a positive constant ω and non-negative v [63]. The model (19) thus turns into

$$f(\mathcal{R}, T^2) = \mathcal{R} - v\omega \tanh(\varphi) + \beta T^2, \quad (24)$$

where $\varphi = \frac{\mathcal{R}}{\omega}$. Combining the above model with Eqs.(16)-(18), we obtain

$$\rho^{eff} = \frac{1}{1 - v \sec h^2 \varphi} \left[\frac{v\omega}{2} \tanh^2 \varphi + \frac{3m}{4\pi r^3} + \frac{\beta m^2}{48\pi^2 r^6} (54 + 33\varsigma + 4\varsigma^2) - \frac{v\mathcal{R}}{2} \right. \\ \left. \times \sec h^2 \varphi + \frac{7 - B^2 r^4 - 10Br^2}{7(1+Br^2)^2} \left\{ \frac{v \sec h^4 \varphi}{\omega^2} (2 - 4 \tanh^2 \varphi) \mathcal{R}'^2 + \frac{\sec h^4 \varphi}{\omega} \right. \right. \\ \left. \left. \times v \left(\mathcal{R}'' - \mathcal{R}' \left(\frac{8Br(-3+Br^2)}{(1+Br)(10Br^2-7+B^2r^4)} - \frac{2}{r} \right) \right) \right\} \right], \quad (25)$$

$$P_r^{eff} = \frac{1}{1 - v \sec h^2 \varphi} \left[\frac{\beta m^2}{48\pi^2 r^6} (18 + 7\varsigma - 4\varsigma^2) + \frac{m}{4\pi r^3} + v \sec h^2 \varphi \left\{ \frac{\mathcal{R}}{2} \right. \right. \\ \left. \left. - \frac{7 - B^2 r^4 - 10Br^2}{7(1+Br^2)^2} \left(\frac{4Br}{1+Br^2} + \frac{2}{r} \right) \frac{2 \tanh \varphi \mathcal{R}'}{\omega} \right\} - \frac{v\omega}{2} \tanh \varphi \right], \quad (26)$$

$$P_t^{eff} = \frac{1}{1 - v \sec h^2 \varphi} \left[\frac{\beta m^2}{16\pi^2 r^6} \left(6 + \frac{1}{3}\varsigma \right) + (1+\varsigma) \frac{m}{4\pi r^3} - \frac{7 - B^2 r^4 - 10Br^2}{7(1+Br^2)^2} \right. \\ \left. \times \left\{ (2 - 4 \tanh^2 \varphi) \mathcal{R}'^2 + \omega \sinh 2\varphi \left(\mathcal{R}'' + \mathcal{R}' \left(\frac{4Br}{1+Br^2} - \frac{8Br}{(1+Br)} \right) \right) \right\} \right]$$

$$\times \frac{(Br^2 - 3)}{(10Br^2 - 7 + B^2r^4) + \frac{1}{r}} \left. \right\} \frac{v \sec h^4 \varphi}{\omega^2} - \frac{v\omega}{2} \tanh \varphi + \frac{v\mathcal{R}}{2} \sec h^2 \varphi \Big]. \quad (27)$$

4 Physical Features of Stellar Objects

In this section, we explore some physical features of the considered anisotropic star candidates through graphical analysis. We investigate varying profiles of several parameters including the effective matter determinants, EoS parameters, viability conditions, surface redshift and compactness within the interior of stars for both models I and II by choosing $\alpha = 0.1$, $\beta = 0.2$, $\varsigma = 1.5$, $v = 0.01$ and $\omega = 0.2$. Furthermore, the stability shall be evaluated through the sound speed and cracking approaches in the next section.

Here, we opt to fix the model parameters as a methodological choice to maintain a focused exploration of the anisotropic star solutions in modified gravity. The decision to set these parameters as constants is primarily motivated by the desire to isolate the effects of anisotropy and modified gravity on the star's structure. While we acknowledge that alternative approaches, such as constraining the parameter values through energy conditions or other information, are valid and have been employed in various studies, our decision to fix the parameters is in line with certain methodological precedents within the literature. We have observed that similar analysis in the field often adopt this approach to simplify the investigation and draw clearer conclusions about the specific aspects under consideration.

4.1 Effective Matter Determinants

Fluid parameters are fundamental quantities used to describe and characterize the behavior of matter in celestial objects such as stars and galaxies. They must be maximum in the core and exhibit a gradually decreasing profile as we approach to the surface of neutron stars. This behavior is a direct consequence of the dense nature of these stellar objects. The graphical representation in Figure 2 illustrates that the effective energy density and pressure components possess a well-agreed trend corresponding to both modified models. Furthermore, their derivatives with respect to the radial coordinate are shown to be consistent with the regular conditions. Their graphs are provided in Figure 3.

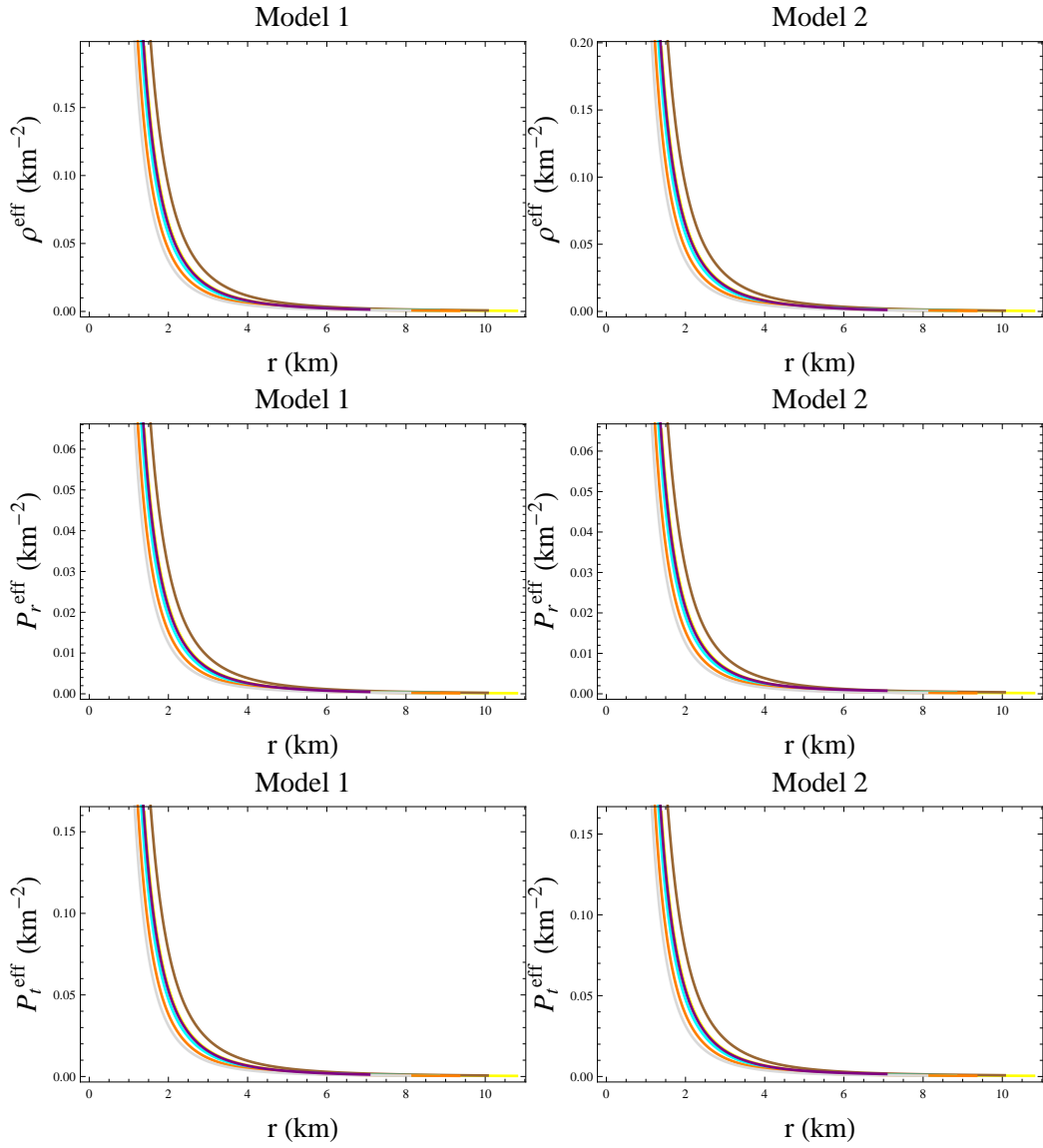


Figure 2: Effective matter determinants versus r corresponding to SMC X-1 (orange), PSR J0348-0432 (brown), Her X-1 (gray), LMC X-4 (cyan), Cen X-3 (yellow) and SAX J 1808.4-3658 (purple).

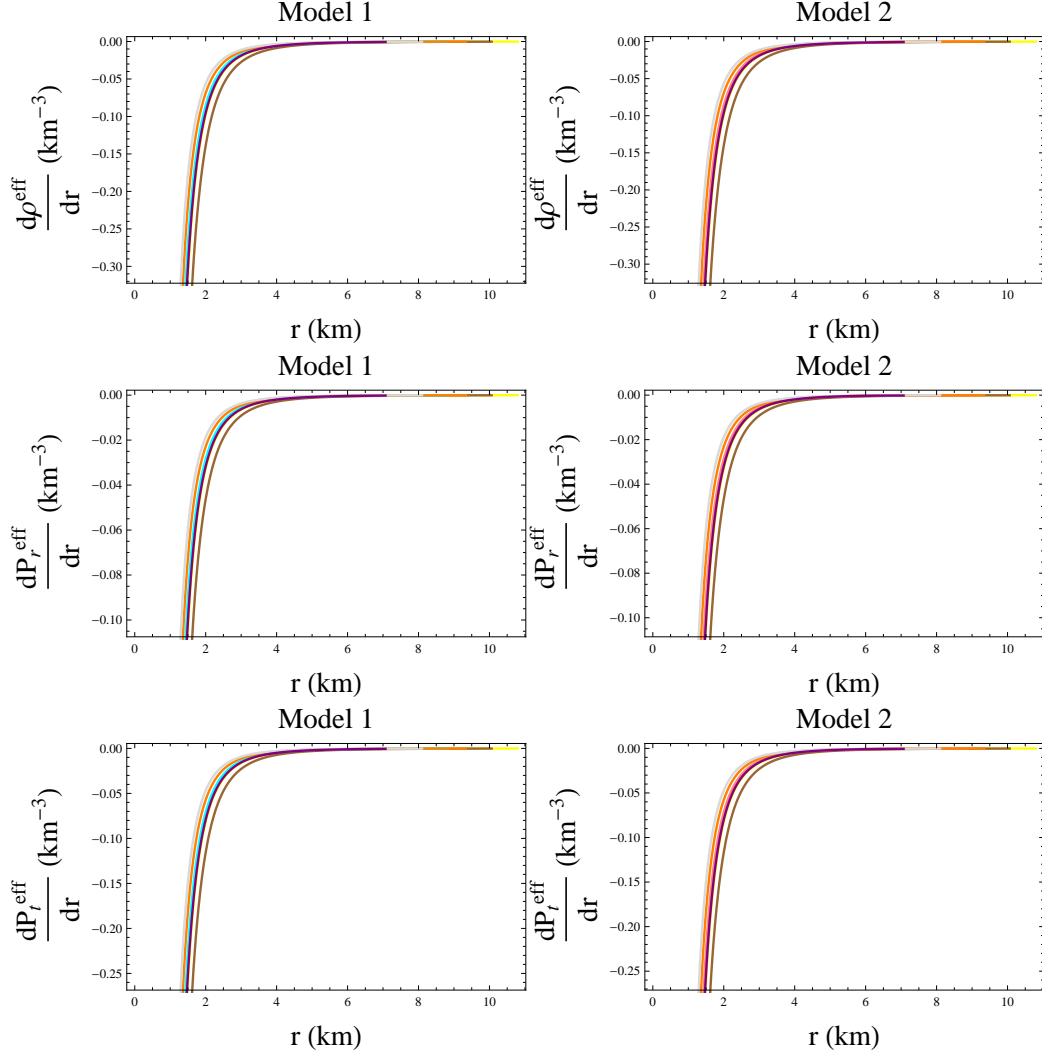


Figure 3: Gradients of effective matter determinants versus r corresponding to SMC X-1 (orange), PSR J0348-0432 (brown), Her X-1 (gray), LMC X-4 (cyan), Cen X-3 (yellow) and SAX J 1808.4-3658 (purple).

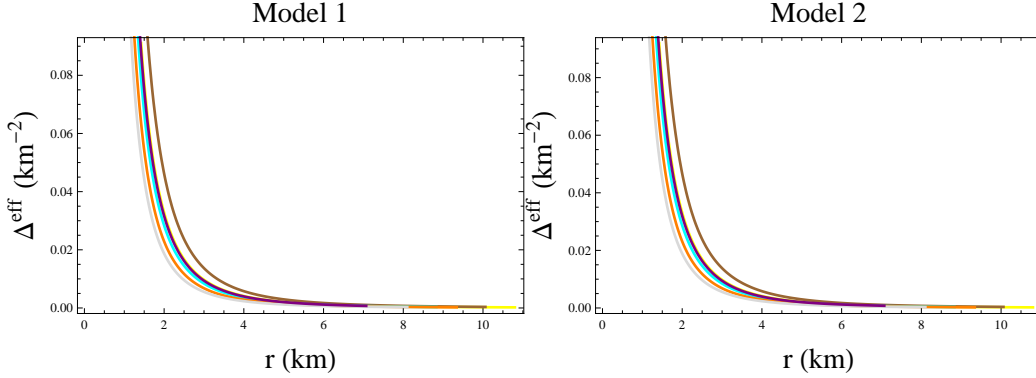


Figure 4: Anisotropic factor versus r corresponding to SMC X-1 (orange), PSR J0348-0432 (brown), Her X-1 (gray), LMC X-4 (cyan), Cen X-3 (yellow) and SAX J 1808.4-3658 (purple).

4.2 Anisotropy

Anisotropy means pressure within the system varies with respect to the direction along which it is measured. Determining whether the anisotropic pressure is positive or negative is a crucial factor in discussing the stability of stellar objects.

- When the anisotropy is positive, it indicates that pressure is directed outward from the center of the system, counterbalancing the inward-directed gravitational force. This phenomenon can be observed in various physical systems, such as stars or in other bodies where the pressure acts to expand or push outward in specific directions.
- When the anisotropy is negative, it produces the inward-directed pressure that would lead to unstable objects. Negative anisotropy is observed in situations where the pressure acts to contract or pull inward along certain axes within the system.

In Figure 4, the anisotropy ($\Delta^{eff} = P_t^{eff} - P_r^{eff}$) is positively oriented, indicating a situation where the pressure within the system exerts an outward force.

4.3 Energy Conditions

The energy conditions are of great importance because they help in determining the nature of the matter within the self-gravitating interior. For instance, their fulfillment confirms that the interior must hold an ordinary matter, otherwise, it exhibits some exotic properties. Additionally, they are used to check the viability of the solutions to the field equations. In other words, these conditions allow researchers to study whether the developed theoretical solutions in GR or other modified theories are physically realistic or not. The energy conditions are categorized as null *NECs*, strong *SECs*, dominant *DECs* and weak *WECs* defined as

- *NECs*

$$0 \leq P_r^{eff} + \rho^{eff}, \quad 0 \leq P_t^{eff} + \rho^{eff},$$

- *SECs*

$$0 \leq P_r^{eff} + \rho^{eff}, \quad 0 \leq P_t^{eff} + \rho^{eff}, \quad 0 \leq 2P_t^{eff} + P_r^{eff} + \rho^{eff},$$

- *DECs*

$$0 \leq \rho^{eff} \pm P_r^{eff}, \quad 0 \leq \rho^{eff} \pm P_t^{eff},$$

- *WECs*

$$0 \leq \rho^{eff}, \quad 0 \leq \rho^{eff} + P_t^{eff}, \quad 0 \leq \rho^{eff} + P_r^{eff}.$$

Figures 5 and 6 provide clear evidence that the considered stars have the characteristics of an ordinary matter, as all the energy constraints are fulfilled.

4.4 Equation of State Parameters

Here, we analyze some parameters to understand the relationship between different fluid parameters within a system. An important criteria for a physically feasible stellar model is that its EoS parameters fall within the range $[0, 1]$. Figure 7 shows that the radial ω_r^{eff} and tangential ω_t^{eff} parameters defined below meet the required condition

$$\omega_r^{eff} = \frac{P_r^{eff}}{\rho^{eff}}, \quad \omega_t^{eff} = \frac{P_t^{eff}}{\rho^{eff}}.$$

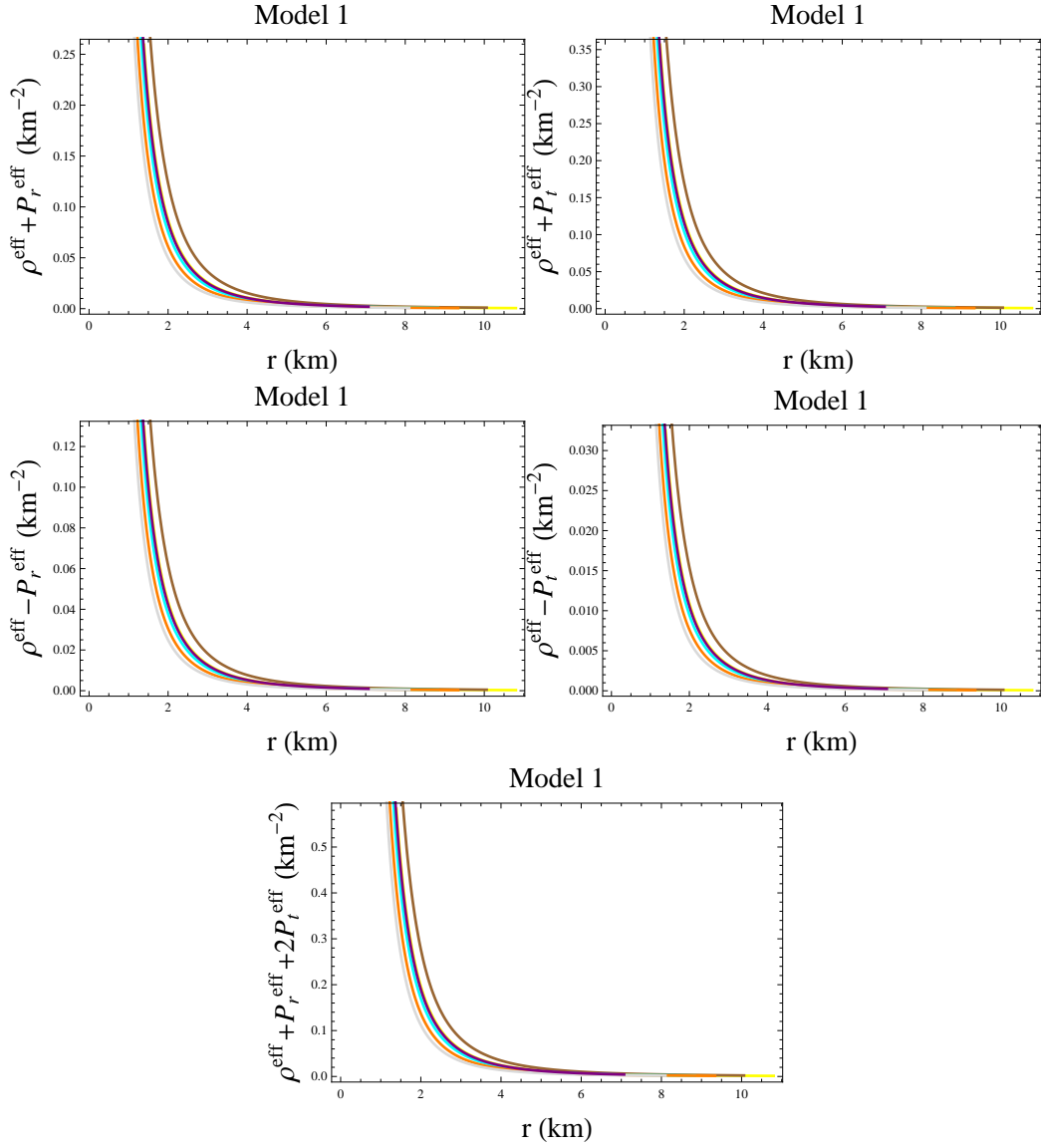


Figure 5: Energy bounds versus r corresponding to SMC X-1 (orange), PSR J0348-0432 (brown), Her X-1 (gray), LMC X-4 (cyan), Cen X-3 (yellow) and SAX J 1808.4-3658 (purple).

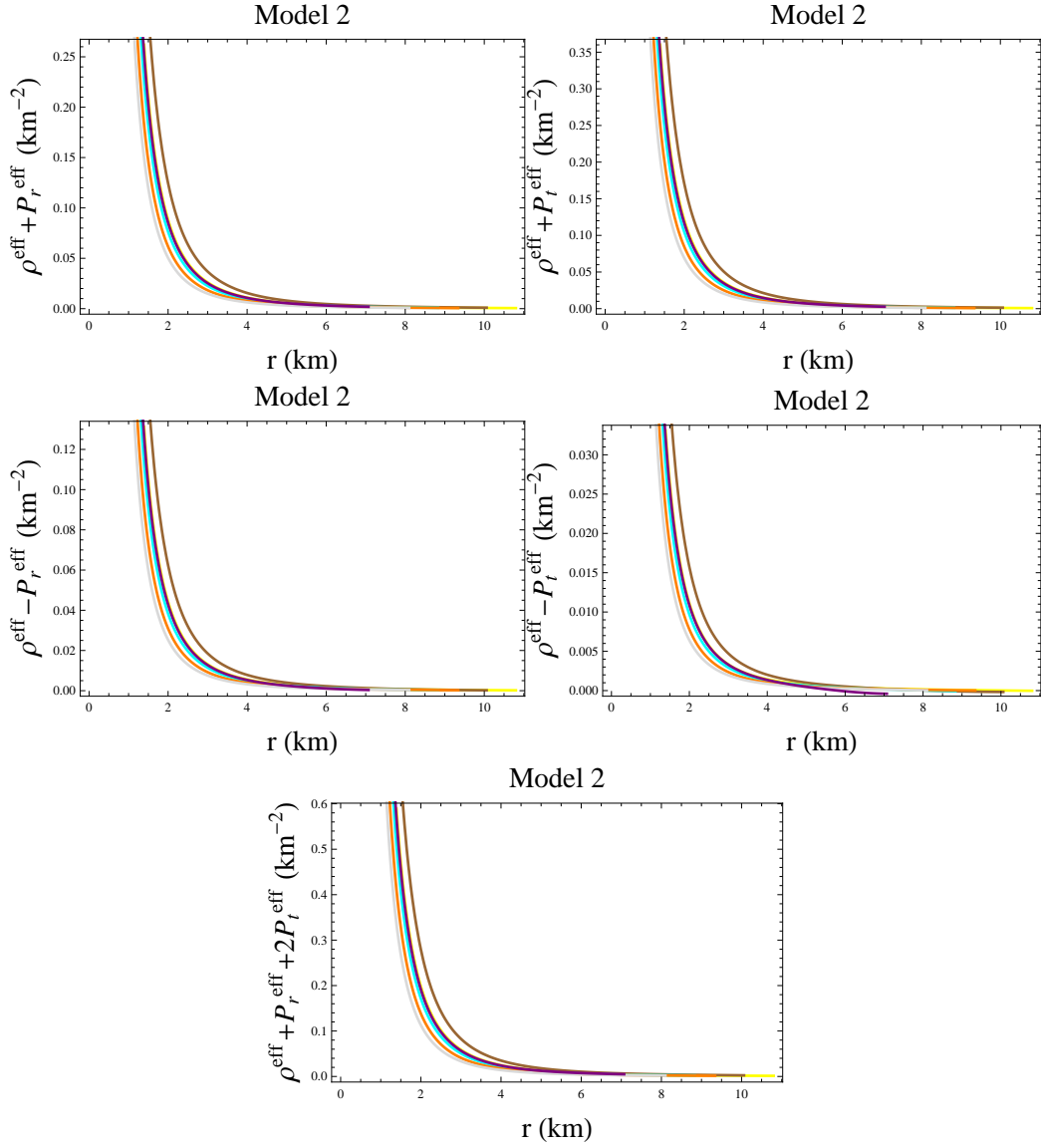


Figure 6: Energy bounds versus r corresponding to SMC X-1 (orange), PSR J0348-0432 (brown), Her X-1 (gray), LMC X-4 (cyan), Cen X-3 (yellow) and SAX J 1808.4-3658 (purple).

Saes and Mendes [64] described some interesting and useful properties of the stiffness of nuclear matter through a particular EoS and discussed its consequences in contempt of current as well as future observations regarding neutron stars.

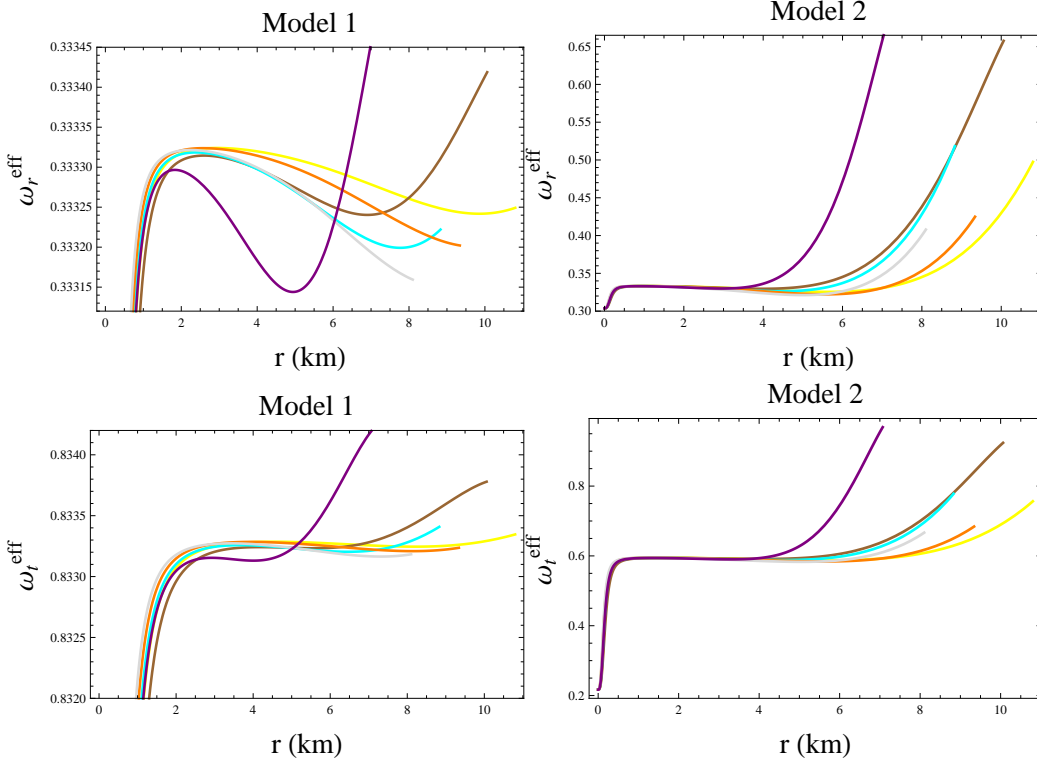


Figure 7: EoS parameters versus r corresponding to SMC X-1 (orange), PSR J0348-0432 (brown), Her X-1 (gray), LMC X-4 (cyan), Cen X-3 (yellow) and SAX J 1808.4-3658 (purple).

4.5 Mass, Compactness and Redshift

Mass represents the total amount of matter contained within a given volume or object. In stars, the mass is a fundamental parameter that influences gravitational forces, determining the overall structure and dynamics of that

object. Mathematically, it is given as

$$m(r) = \frac{1}{2} \int_0^R r^2 \rho^{eff} dr. \quad (28)$$

Figure 8 illustrates a positive correlation between mass and radius, indicating that as the radius of the star increases, its mass also increases. Compactness is a dimensionless parameter often used to describe how tightly matter is packed within a celestial object. It is defined as the ratio of mass to the object size (typically expressed as its radius). This factor plays a role in determining whether a celestial object will form a black hole after collapsing or not. It can be expressed as

$$u(r) = \frac{m(r)}{r}. \quad (29)$$

There is a specific limit for this factor proposed by Buchdhal [65] while discussing a physically relevant model. According to him, this ratio should be less than $\frac{4}{9}$ everywhere. If this ratio exceeds the suggested limit, then the structure may find to be too dense or concentrated within its given radius, which could lead to potential instability or collapse.

In cosmology, redshift is a measure of how much the light emitted by distant objects has been stretched due to the expansion of the universe. It provides crucial information about the relative motion of celestial objects and is helpful in studying the large-scale structures and expansion of the universe. We define it as follows

$$Z_s = \frac{1}{\sqrt{1 - 2u(r)}} - 1. \quad (30)$$

For a physically viable model, the redshift must be $Z_s \leq 5.2$ [66]. Figure 8 shows plots of these two factors which are consistent with their respective findings.

5 Stability Analysis

Stability is a fundamental concept to ensure the existence of celestial objects. It becomes appealing to analyze the celestial bodies that manage to maintain their stability even when subjected to the external disturbances. In the realm of astrophysics, the investigation of a star's stability often involves two important notions, i.e., the sound speed, the cracking criterion and the adiabatic index.

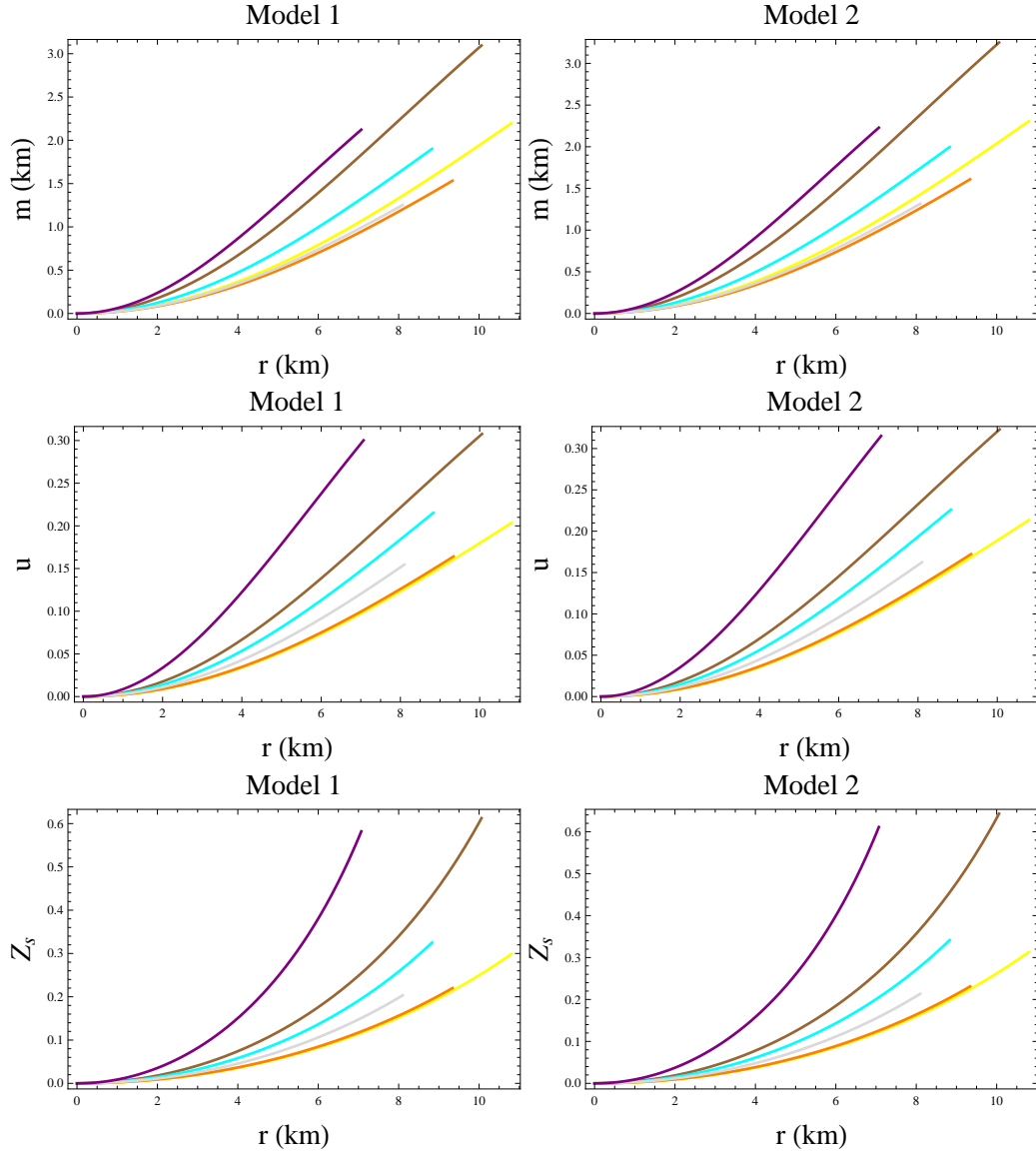


Figure 8: Mass, compactness and redshift function versus r corresponding to SMC X-1 (orange), PSR J0348-0432 (brown), Her X-1 (gray), LMC X-4 (cyan), Cen X-3 (yellow) and SAX J 1808.4-3658 (purple).

5.1 Sound Speed

Sound speed refers to the speed at which pressure waves (sound waves) propagate through a medium. In the context of stars, sound speed is a key indicator of how effectively pressure can counteract gravitational forces. A stable star should have a sound speed sufficient to maintain its structural integrity, preventing it from the gravitational collapse. It also helps researchers to understand how disturbances propagate within the star and whether they lead to instability. According to the causality condition, it is necessary that both the radial $v_r^{2(eff)}$ and transverse $v_t^{2(eff)}$ components

$$v_r^{2(eff)} = \frac{dP_r^{eff}}{d\rho^{eff}}, \quad v_t^{2(eff)} = \frac{dP_t^{eff}}{d\rho^{eff}},$$

lie within the range of $(0, 1)$ to get a stable interior. The fulfilment of this criterion is verified in Figure 9.

5.2 Herrera's Cracking Approach

The cracking approach is a theoretical framework pioneered by Herrera and his colleagues [67] to examine the stability of self-gravitating systems. The interaction of pressure gradients with the force of gravity produces instabilities in the system, leading to the occurrence of cracking phenomenon. According to this technique, a self-gravitating system can be considered stable only when the difference between the radial and transverse components of the sound speed should be in between 0 and 1. The failure of this condition implies instability within the system, potentially leading to a catastrophic collapse. Figure 9 ensures the stability of all our considered stars (lower two plots).

5.3 Adiabatic Index

The adiabatic index is an important parameter used to study the stability of self-gravitating objects. Stars are considered to be in equilibrium state, where the inward force of gravity is counterbalanced by the outward pressure generated by heat and radiation inside the star. The stability of a star depends on the balance between these two forces and the adiabatic index is a key factor in determining the pressure force. According to Heintzmann

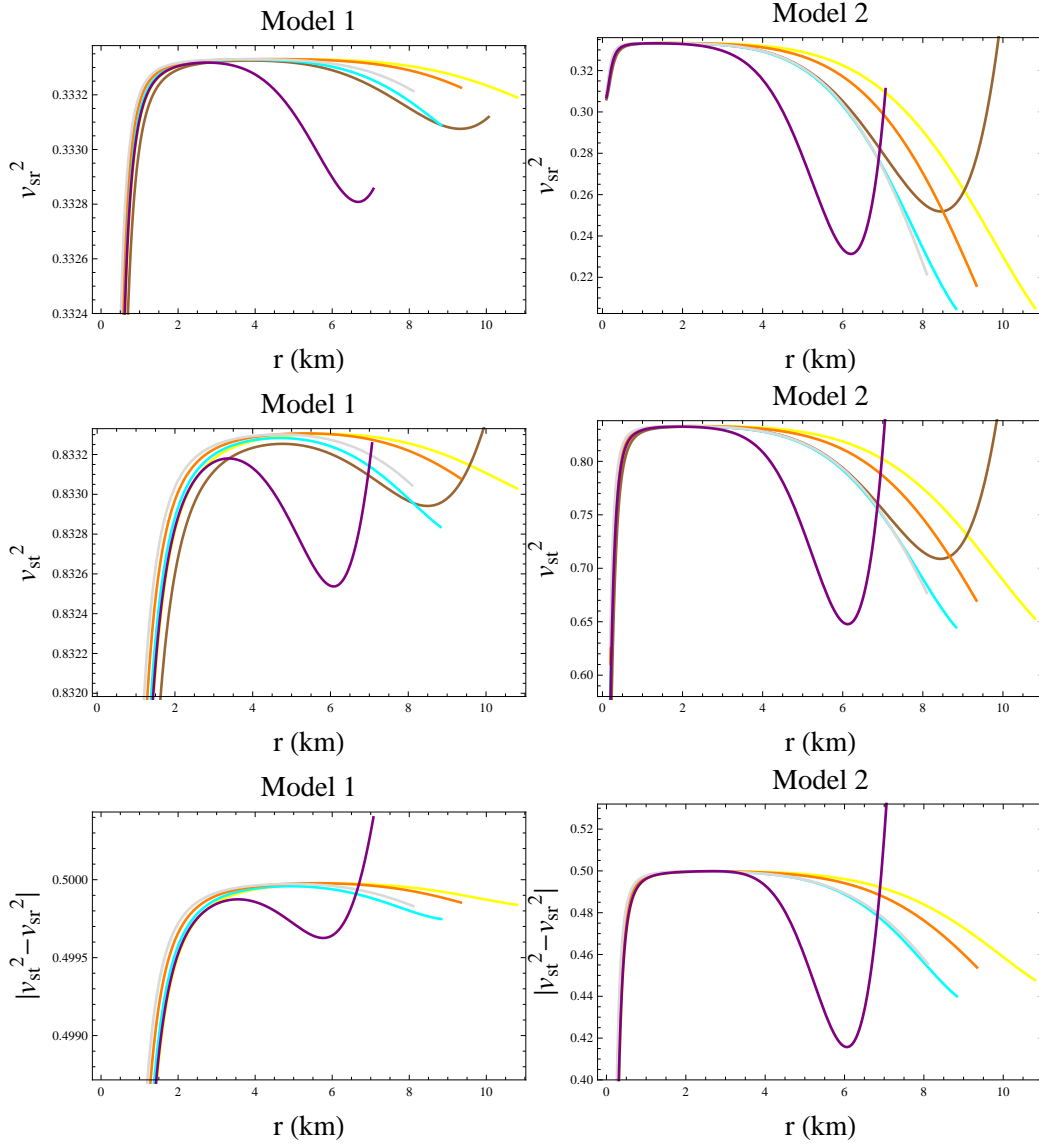


Figure 9: Speed of sound and cracking versus r corresponding to SMC X-1 (orange), PSR J0348-0432 (brown), Her X-1 (gray), LMC X-4 (cyan), Cen X-3 (yellow) and SAX J 1808.4-3658 (purple).

and Hillebrandt [68], if the radial and transverse components, respectively,

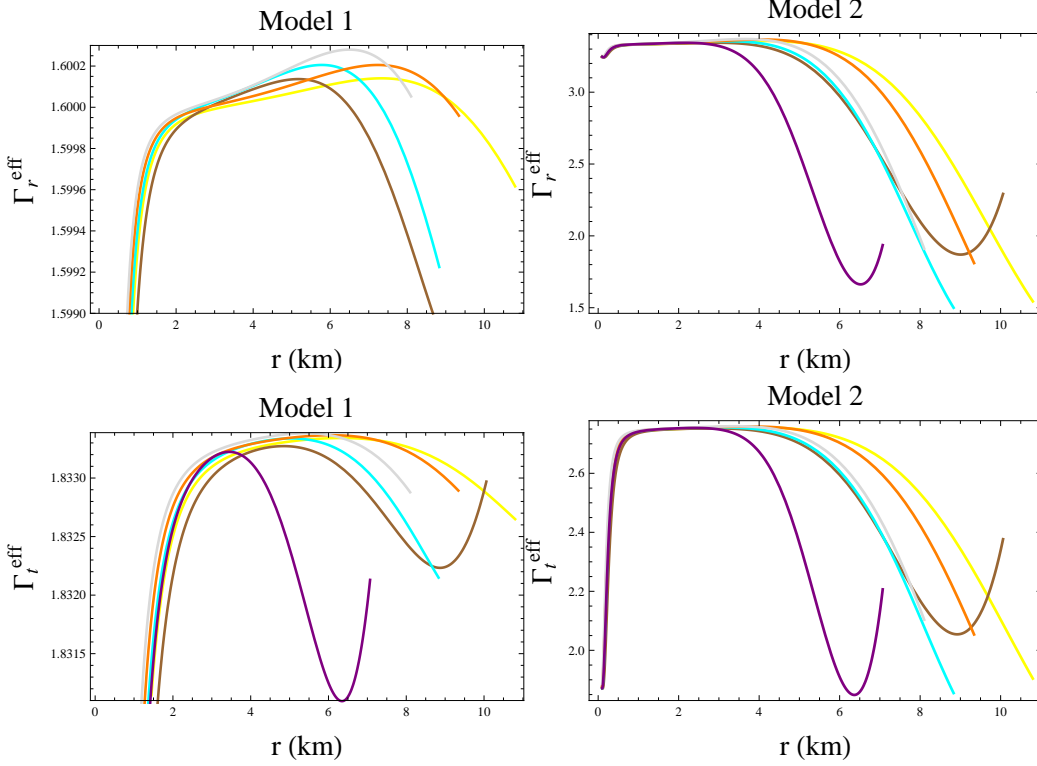


Figure 10: Adiabatic index versus r corresponding to SMC X-1 (orange), PSR J0348-0432 (brown), Her X-1 (gray), LMC X-4 (cyan), Cen X-3 (yellow) and SAX J 1808.4-3658 (purple).

defined by

$$\Gamma_r^{eff} = \frac{\rho^{eff} + P_r^{eff}}{P_r^{eff}} \frac{dP_r^{eff}}{d\rho^{eff}}, \quad \Gamma_t^{eff} = \frac{\rho^{eff} + P_t^{eff}}{P_t^{eff}} \frac{dP_t^{eff}}{d\rho^{eff}},$$

are greater than $\frac{4}{3}$, then a perturbation compressing the star will cause an increase in pressure that resists the compression leading to a stable star. However, if the components of adiabatic index are less than the defined limit, then the compression will cause a decrease in pressure leading to further compression and instability. Figure 10 shows our considered stars to be stable.

6 Final Remarks

This paper is devoted to the formulation of Durgapal-Fuloria anisotropic solutions in the background of $f(\mathcal{R}, T^2)$ gravity. In order to do this, a static spherical interior metric and the anisotropic energy-momentum tensor have been considered. The corresponding modified field equations have then been developed, containing extra degrees of freedom. We have tackled with these equations by considering the Durgapal-Fuloria metric possessing two constants (A, B) . These unknowns have been calculated through matching conditions between the interior and Schwarzschild exterior spacetimes. Further, we have taken two different minimal models of this modified theory and analyzed the physical behavior of our considered stars by examining the resulting matter variables, anisotropy, energy conditions and stability. The summary of our obtained results is presented as follows.

- Both the metric potentials are positive and exhibit increasing profile. They show minimum value at the core of stars and monotonically increasing behavior as we move towards the spherical interface (Figure 1).
- The effective matter variables reach their highest values at $r = 0$ and gradually decrease outwards (Figure 2). The derivatives of these effective parameters indicate the presence of dense neutron stars (Figure 3).
- The positive anisotropy manifests the presence of a repulsive force essential for the stability of neutron objects (Figure 4).
- All energy constraints are satisfied providing a strong evidence of the viability of our developed solutions. They also signify that the interior of stellar objects primarily consists of an ordinary matter (Figures 5 and 6).
- Our considered models are consistent as the EoS parameters lie within the range $[0, 1]$ (Figure 7).
- The behavior of mass function, compactness and redshift functions have also found to be within their required limits (Figure 8).
- Deriving the Tolman-Oppenheimer-Volkoff (TOV) equations for our formulated models is a subject of great discussion when discussing the

neutron stars. However, we would like to mention the inherent limitations of the modified gravitational theory we are working within. Unfortunately, the specific form of the theory we are investigating does not readily provide the graphical profiles of the energy density and pressure components at the center of the massive star unlike $f(\mathcal{R}, T)$ [69] and $f(\mathcal{R}, T, \mathcal{Q})$ (where $\mathcal{Q} \equiv \mathcal{R}_{\xi\psi} T^{\xi\psi}$) [70] theories. This limitation arises from the intricate nature of the theory, and as a result, constructing plots of the TOV equations may not be feasible within the scope of this study.

- All the stability requirements have been satisfied for chosen parametric values (Figures 9 and 10).

It is important to mention here that the values of all physical parameters in this theory increase as compared to GR [71, 72] and other modified theories. We conclude that our considered neutron stars are physically viable and stable for both $f(\mathcal{R}, T^2)$ models.

Data Availability Statement: This manuscript has no associated data.

References

- [1] Shafi, Q. and Wetterich, C.: Phys. Lett. B **129**(1983)387.
- [2] Capozziello, S.: Int. J. Mod. Phys. D **483**(2002)11; Nojiri, S. and Odintsov, S.D.: Phys. Rev. D **68**(2003)123512.
- [3] Nobleson, K., Banik, S. and Malik, T.: Phys. Rev. D **107**(2023)124045.
- [4] Harko, T. et al.: Phys. Rev. D **84**(2011)024020.
- [5] Naseer, T. and Sharif, M.: Fortschr. Phys. **71**(2023)230004;
- [6] Sharif, M. and Naseer, T.: Eur. Phys. J. Plus **137**(2022)1304.
- [7] Crisostomi, M., Koyama, K. and Tasinato, G.: J. Cosmol. Astropart. Phys. **04**(2016)044.
- [8] Katirci, N. and Kavuk, M.: Eur. Phys. J. Plus **129**(2014)163.
- [9] Board, C.V.R. and Barrow, J.D.: Phys. Rev. D **96**(2017)123517.

- [10] Moraes, P.H.R.S. and Sahoo, P.K.: Phys. Rev. D **97**(2018)024007.
- [11] Alam, N. et al.: arXiv:2309.06022v1.
- [12] Dev, K. and Gleiser, M.: Gen. Relativ. Gravit. **34**(2002)1793;
35(2003)1435.
- [13] Mak, M.K. and Harko, T.: Proc. R. Soc. Lond. A **459**(2003)393.
- [14] Kalam, M. et al.: Eur. Phys. J. C **72**(2012)2248.
- [15] Alam, N. et al.: Phys. Rev. C **94**(2016)052801.
- [16] Malik, T. et al.: Phys. Rev. C **98**(2018)035804.
- [17] Singh, K.N. and Pant, N.: Eur. Phys. J. C **76**(2016)524.
- [18] Maurya, S.K. and Ortiz, F.: Ann. Phys. **414**(2020)168070.
- [19] Sharif, M. and Naseer, T.: Phys. Scr. **97**(2022)055004.
- [20] Sharif, M. and Naseer, T.: Fortschr. Phys. **71**(2023)2200147.
- [21] Sharif, M. and Naseer, T.: Phys. Scr. **98**(2023)105009.
- [22] Herrera, L., Di Prisco, A. and Ospino, J.: Phys. Rev. D **74**(2006)044001.
- [23] Herrera, L. and Barreto, W.: Phys. Rev. D **88**(2013)084022.
- [24] Abbott, B.P. et al.: Phys. Rev. Lett. **119**(2017)161101.
- [25] Maurya, S.K., Banerjee, A. and Hansraj, S.: Phys. Rev. D **97**(2018)044022.
- [26] Pretel, J.M.Z. and da Silva, M.F.A.: Gen. Relativ. Gravit. **51**(2019)3.
- [27] Pretel, J.M.Z.: Eur. Phys. J. C **80**(2020)726.
- [28] Pretel, J.M.Z. and da Silva, M.F.A.: Mon. Not. R. Astron. Soc. **495**(2020)5027.
- [29] Arbañil, J.D.V. and Moraes, P.H.R.S.: Eur. Phys. J. Plus **135**(2020)354.
- [30] Negi, P.S.: Int. J. Theor. Phys. **45**(2006)1684.

- [31] Stephani, H. et al.: *Exact solutions of Einstein's field equations* (Cambridge University Press, New York, 2009).
- [32] Semiz, I.: Rev. Math. Phys. **23**(2011)865.
- [33] Ruderman, R.: Ann. Rev. Astron. Astrophys. **10**(1972)427.
- [34] Ovalle, J.: Mod. Phys. Lett. A **23**(2008)3247.
- [35] Germani, C. and Maartens, R.: Phys. Rev. D **64**(2001)124010.
- [36] Ovalle, J., Gergely, L.A. and Casadio, R.: Class. Quantum Grav. **32**(2015)045015.
- [37] Maurya, S.K. et al.: Astrophys. Space Sci. **361**(2016)163.
- [38] Cho, I. and Kim, H.C.: Chin. Phys. C **43**(2019)025101.
- [39] Rahmansyah, A. et al.: Eur. Phys. J. C **80**(2020)769.
- [40] Rahmansyah, A. and Sulaksono, A.: Phys. Rev. C **104**(2021)065805.
- [41] Danarianto, M.D. and Sulaksono, A.: Phys. Rev. D **100**(2019)064042.
- [42] Rahmansyah, A. et al.: Phys. Rev. D **106**(2022)084042.
- [43] Prasetyo, I. et al.: Eur. Phys. J. C **82**(2022)884.
- [44] Rizaldy, R. and Sulaksono, A.: Phys. Rev. C **109**(2024)025803.
- [45] Bogdanov, S. et al.: Astrophys. J. Lett. **887**(2019)L25.
- [46] Danilenko, A. et al.: Mon. Not. R. Astron. Soc. **493**(2020)1874.
- [47] Prasetyo, I. et al.: Phys. Rev. D **104**(2021)084029.
- [48] Li, A. et al.: Astrophys. J. **913**(2021)27.
- [49] Durgapal, M.C. and Fuloria, R.S.: Gen. Relativ. Gravit. **17**(1985)671.
- [50] Maurya, S.K. et al.: Eur. Phys. J. C **75**(2015)225.
- [51] Komathiraj, K. et al.: J. Astrophys. Astron. **40**(2019)15.
- [52] Maurya, S.K. et al.: Phys. Dark Universe **42**(2023)101284.

- [53] Abubekerov, M.K. et al.: *Astron. Rep.* **52**(2008)379.
- [54] Rawls, M.L. et al.: *Astrophys. J.* **730**(2011)25.
- [55] Li, X.D. et al.: *Phys. Rev. Lett.* **83**(1999)3776.
- [56] Zubair, M., Abbas, G. and Noureen, I.: *Astrophys. Space Sci.* **361**(2016)8.
- [57] Nashed, G.G.L. and Capozziello, S.: *Eur. Phys. J. C* **81**(2021)481.
- [58] Zhao, Y. et al.: *Mater. Des.* **216**(2022)110555.
- [59] Zhang, Y. et al.: *ACS Appl. Mater. Interfaces* **15**(2023)32984.
- [60] Shi, Y. et al.: *AIAA J.* **61**(2023)3404.
- [61] Gao, J. et al.: *Opt. Express* **31**(2023)44703.
- [62] Starobinsky, A.A.: *Phys. Lett. B* **91**(1980)99.
- [63] Tsujikawa, S.: *Phys. Rev. D* **77**(2008)023507.
- [64] Saes, J.A. and Mendes, R.F.P.: *Phys. Rev. D* **106**(2022)043027.
- [65] Buchdahl, A.H.: *Phys. Rev. D* **116**(1959)1027.
- [66] Ivanov, B.V.: *Phys. Rev. D* **65**(2002)104011.
- [67] Herrera, L.: *Phys. Lett. A* **165**(1992)206.
- [68] Heintzmann, H. and Hillebrandt, W.: *Astron. Astrophys.* **38**(1975)51.
- [69] Errehymy, A. et al.: *Chin. J. Phys.* **77**(2022)1502.
- [70] Naseer, T. and Sharif, M.: *Chin. J. Phys.* **88**(2024)10.
- [71] Deb, D. et al.: *Ann. Phys.* **387**(2017)239.
- [72] Singh, K.N. et al.: *Eur. Phys. J. A* **53**(2017)21.